HHS Public Access

Author manuscript

J Bioenerg Biomembr. Author manuscript; available in PMC 2014 June 11.

Published in final edited form as:

J Bioenerg Biomembr. 2013 February ; 45(0): 101–109. doi:10.1007/s10863-012-9477-5.

Early alterations in mitochondrial reserve capacity; a means to predict subsequent photoreceptor cell death

Nathan R. Perron,

Departments of Pharmaceutical Sciences, Medical University of South Carolina, Charleston, SC 29425, USA

Craig Beeson, and

Departments of Pharmaceutical Sciences, Medical University of South Carolina, Charleston, SC 29425, USA

College of Pharmacy/Pharmaceutical & Biomedical Sciences, Medical University of South Carolina, 280 Calhoun Street, Charleston, SC 29425, USA, beesonc@musc.edu

Bärbel Rohrer

Departments of Ophthalmology, Medical University of South Carolina, 167 Ashley Ave, SEI 511, Charleston, SC 29425, USA, rohrer@musc.edu

Departments of Research Service, Ralph H Johnson VA Medical Center, Charleston, SC 29425, USA

Abstract

Although genetic and environmental factors contribute to neurodegenerative disease, the underlying etiology common to many diseases might be based on metabolic demand. Mitochondria are the main producer of ATP, but are also the major source of reactive oxygen species. Under normal conditions, these oxidants are neutralized; however, under environmental insult or genetic susceptibility conditions, oxidative stress may exceed cellular antioxidant capacities, leading to degeneration. We tested the hypothesis that loss in mitochondrial reserve capacity plays a causative role in neuronal degeneration and chose a cone photoreceptor cell line as our model. 661W cells were exposed to agents that mimic oxidant stress or calcium overload. Real-time changes in cellular metabolism were assessed using the multi-well Seahorse Biosciences XF24 analyzer that measures oxygen consumption (OCR) and extracellular acidification rates (ECAR). Cellular stress resulted in an early loss of mitochondrial reserve capacity, without affecting basal respiration; and ECAR was increased, representing a compensatory shift of ATP productions toward glycolysis. The degree of change in energy metabolism was correlated with the amount of subsequent cell death 24-hours post-treatment, the concentration-dependent loss in mitochondrial reserve capacity correlated with the number of live cells. Our data suggested first, that loss in mitochondrial reserve capacity is a major contributor in disease pathogenesis; and second, that the XF24 assay might represent a useful surrogate assay

Correspondence to: Craig Beeson; Bärbel Rohrer.

amenable to the screening of agents that protect against loss of mitochondrial reserve capacity. In future experiments, we will explore these concepts for the development of neuroprotective agents.

Keywords

Mitochondrial respiration; Cell death; Photoreceptors; Retinitis pigmentosa

Introduction

Although genetic and environmental factors contribute to the pathology in neurodegenerative diseases, the underlying etiology common to many of these diseases arises from the extreme high energy demand of the central nervous system. Mitochondria produce reactive oxygen species (ROS) that are typically well-tolerated under homeostatic conditions, but when mitochondrial damage occurs, oxidative stress may overwhelm the antioxidant capacity, causing degeneration and cell death.

As a model system we picked a photoreceptor cell line (661W) (Tan et al. 2004), since there is increasing evidence that the retina's high metabolic demand and mitochondrial content, together with the presence of oxidative stressors generated in part by light (Cruickshanks et al. 1993; Grimm et al. 2000; Krishnamoorthy et al. 1999), cause persistent mitochondrial damage in the retina. Mitochondrial dysfunction within retina cells elevates the rate of ROS production due to damage of the electron transport chain (ETC) proteins, and also to the mitochondrial DNA (mtDNA) that encodes some of the ETC protein subunits (Jarrett et al. 2008). Diminished mitochondrial function reduces the rate of ATP production causing reduced activity of the plasma membrane Na^+-K^+ ATPase. Because extrusion of calcium from the cytoplasm partly depends on the Na^+-dependent calcium exchanger, reduced Na^+-K^+ ATPase activity results in elevated intracellular calcium. Sustained, increased levels of intracellular calcium also cause mitochondrial stress due to activation of ETC flux, and mitochondrial swelling (Yoshida et al. 1992). Eventually, elevated calcium leads to mitochondrial failure and apoptosis as has been shown in the *rd1* model of retinitis pigmentosa (RP) (Fox et al. 1999; Sharma and Rohrer 2004) as well as other neurodegenerative diseases (Zglinicki 2003) and perhaps aging (Beckman and Ames 1998; Brand 2000; Brand and Nicholls 2011). Loss of mitochondrial reserve capacity in response to elevated ROS levels has also been demonstrated with the Seahorse Biosciences extracellular flux instrument in cellular models of renal, cardiovascular, and neurodegenerative diseases (Dranka et al. 2010, 2011), as well as in MERRF syndrome using isolated skin fibroblasts (Wu and Wei 2012).

Glycolysis can partly compensate for the loss or decrease of ATP production following mitochondrial damage, but maintenance of the NAD^+/NADH redox balance necessitates reduction of pyruvate to lactic acid. Thus, in many tissues, decreased mitochondrial ATP production results in significant increases in glucose uptake and lactate extrusion. This "Pasteur Effect" can be induced in retina cells via addition of a mitochondrial inhibitor such as antimycin A (Fliesler et al. 1997; Winkler et al. 1997, 2000, 2003). Overall, retina cells exhibit profound metabolic plasticity as long as sufficient glucose is available, however,

upon loss of glucose, they die rapidly (Winkler et al. 1997). The 661W cells, a mouse retina tumor-derived cell with cone-photoreceptor cell characteristics (Tan et al. 2004), also display the Pasteur Effect when challenged with hypoxia or mitochondrial inhibitors (Winkler et al. 2004a, b). We have shown that 661W cells treated with compounds to increase intracellular calcium or oxidative stress undergo rapid degeneration (Sharma and Rohrer 2004, 2007).

Although the metabolic effects of calcium or oxidative stress have not been measured directly in isolated mouse photoreceptors or the intact retina, we found that in animal models that exhibit either high calcium or high ROS levels in photoreceptors, their retina expressed high levels of stress and metabolic genes at onset of damage, but expression of the metabolic genes dropped in parallel with the loss of cells (Lohr et al. 2006). Here, we show that both calcium- and oxidative-stress cause mitochondrial dysfunction in 661W cells, revealed as a loss of mitochondrial reserve capacity that precedes any indication of cell death. These results support the hypothesis that loss of mitochondrial reserve capacity has a causative role in retinal neurodegenerative pathologies.

Materials and methods

Reagents

The reagents used in these studies were all tissue culture grade materials and better. Tissue culture materials were all purchased from Invitrogen (Carlsbad, CA) unless otherwise noted. Cell stress was induced using the calcium ionophore, A23187; the oxidant, *tert*-butyl hydroperoxide (*t*BuOOH); the phosphodiesterase inhibitor, 1-isobutyl-4-methylxanthine (IBMX); and the intracellular redox cycler, paraquat (PQ) (all from Sigma-Aldrich, St. Louis, MO).

Cell culture

The 661W cell line used for this study was generously provided by Dr. Muayyad Al-Ubaidi (University of Oklahoma). Cells were grown in Dulbecco's modified-Eagle's medium (DMEM) supplemented with 10 % fetal bovine serum (FBS) in 100 mm tissue culture dishes with cells typically seeded at a concentration between 1×10^5 and 1×10^6 in 10 mL of growth medium. They were allowed to grow to 80 % to 90 % confluence before harvesting for use in experiments.

Dye exclusion assay (live/dead cell fluorescence imaging)

Cells were plated in black-walled 96-well plates with an optically clear tissue culture surface (typically in the range of 10,000–20,000 cells/well) and grown to confluence in DMEM+5 % FBS (~48 h) after which the medium was aspirated, and replaced with DMEM+1 % FBS to arrest cell growth. In this reduced-serum medium, the cells were treated with various stressors (A23187, tBuOOH, IBMX, PQ) at a range of concentrations for 24–48 h. Following treatment, the medium including treatments were aspirated, and the cells were stained for 30 min in the dark with Hoechst 33342 (20 μM) and propidium iodide (7.5 μM) in Dulbecco's phosphate-buffered saline (Sigma-Aldrich) containing 5 mM glucose and 1 % FBS (pH 7.4). Fluorescence images from three fields within each well were taken on the IN

Cell Analyzer 1000 (GE Healthcare, Chalfont St. Giles, United Kingdom) to give the number of dead (propidium iodide-stained, red) cells and the total number of cells (Hoechst-stained, blue) in each well as a function of stressor concentration. The number of dead cells was subtracted from the total number to obtain the number of live cells in each well, which is represented as a percentage of the total number (% live) and is the average of three wells ±SEM. Concentrations of A23187 ranged from 40 nM to 10 μM; concentrations of IBMX and tBuOOH ranged from 80 μM to 10 mM; and PQ concentrations ranged from 80 μM to 20 mM. Control wells receiving no treatment or diluent (respective DMSO concentrations) were also included for comparison.

Extracellular flux: Oxygen Consumption Rate (OCR) and Extracellular Acidification Rate (ECAR) measurements

The OCR and ECAR measurements of 661W cells were performed using a Seahorse Bioscience XF24 instrument (Seahorse Bioscience, Billerica, MD), as initially described by Wu and colleagues (Wu et al. 2007), and more recently by Dranka, et al.(Dranka et al. 2010). O_2-leakage through the plastic sides and bottom of the plate was accounted for using the AKOS algorithm within the XF24 software package. Cells were plated on the 24-well custom plates designed for use in the XF24 (typically 10,000 cells/well) and grown to confluence in DMEM+5 % FBS (~48 h). The medium was then replaced with DMEM+1 % FBS for 24 h (1 % FBS was used instead of 5 % in order to arrest cell growth), along with any treatment. Prior to running the experiment, the growth medium was removed and the cells were washed with PBS containing Ca^{2+}/Mg^{2+} (pH 7.4), which was then aspirated and replaced with 700 μL of reduced serum (RS) buffer. The RS buffer contained $CaCl_2$ (1.8 mM), $MgCl_2$ (0.6 mM), KH_2PO_4 (0.5 mM), KCl (5.33 mM), Na_2HPO_4 (0.5 mM), NaCl (130 mM), glucose (5.6 mM), glutamax, minimum essential medium (MEM) amino acids solution, MEM non-essential amino acids, MEM vitamin solution, penicillin/streptomycin, 1 % bovine serum albumin (BSA, factor V fatty-acid-free), 1 % FBS, and insulin (100 nM). All concentrations are final experimental concentrations and all components except FBS and insulin were combined prior to filter sterilization. Following addition of FBS and insulin (usually 24–48 h pre-experiment), the RS buffer was warmed to 37 °C. Results are presented as the mean±SEM. Each data point represents the average of a group of 3–5 wells per experiment.

Bicinchoninic acid assay for protein content

To assess protein content of cells in experimental wells, the bicinconinic (BCA) protein assay was used as described previously (Redinbaugh and Turley 1986; Smith et al. 1985; Tuszynski and Murphy 1990). To prepare samples for the BCA assay, the growing medium was first aspirated from the cell layer and the cells were washed once with PBS containing Ca^{2+}/Mg^{2+}. Next, the cells were dissolved for a minimum of 4 h at room temperature in 100 μL of either Triton-X or RIPA solubilization buffer. Protein samples were quantified by comparison with a BSA standard calibration curve prepared in the identical solubilization buffer used for cell lysis.

Results

Establishment of the XF24 assay to examine mitochondrial metabolism of 661W cells

Changes in energy metabolism are among the earliest and most informative markers of cellular stress because they arise from the intimate linkage between ATP utilization and most biochemical processes (e.g., membrane integrity, ion balance, protein synthesis, etc.). Assessment of real-time changes in cellular metabolism due to pharmacological interventions has been greatly facilitated with the introduction of the Seahorse Biosciences, XF24 analyzer, which measures oxygen consumption rates (OCR) and extracellular acidification rates (ECAR) for a cell monolayer. After optimizing the 661W cell seeding numbers for the XF24 wells, we evaluated the cellular metabolic capacity and mitochondrial coupling by injecting the following metabolic probes using the liquid injection ports on the XF instrument sensor plate: oligomycin, which inhibits the mitochondrial F_1F_0-ATPase, FCCP (carbonyl cyanide 4-trifluoromethoxy-phenylhydrazone), which is a protonophore that depolarizes the inner mitochondrial membrane, and the mitochondrial ETC inhibitors of complex I (rotenone) and complex III (antimycin A). All mitochondrial probes were individually titrated to identify their minimal effective concentration.

Figure 1 shows the effects of these agents on both OCR (Fig. 1a, closed symbols) and ECAR (Fig. 1a, open symbols). The rapid decrease in OCR upon injection of oligomycin (0.5 μM) indicates that ~50 % of the O_2 consumption is coupled to ATP production. Treatment with FCCP (1 μM) collapses the proton gradient across the inner mitochondrial membrane. The mitochondria increase flux through the electron transport chain in an attempt to restore the proton gradient leading to an immediate increase in OCR. The complex I and III inhibitors, rotenone (500 nM) and antimycin A (500 nM), respectively, block the electron transport chain causing an immediate decrease in OCR that corresponds to the fraction of measured respiration that is mitochondrial oxygen consumption. Any remaining OCR is due to non-mitochondrial sources. As long as substrates for the production of NADH (e.g., pyruvate or palmitic acid) are not rate limiting, the difference between the maximum FCCP-induced increase in OCR and the non-mitochondrial OCR remaining after rotenone+antimycin A inhibition can be referred to as the mitochondrial reserve capacity (Brand et al. 2004; Nichols and Epstein 2009). In 661W cells, the maximal FCCP-uncoupled OCR response usually ranges from 1.5- to 2.5-fold higher than the basal OCR (Fig. 1a) and the increases are not affected by supplementation with 1–3 mM sodium pyruvate or 0.2–0.5 mM palmitic acid (data not shown).

It is notable that because oligomycin blocks mitochondrial ATP production by OXPHOS, it also causes a simultaneous increase in ECAR (Fig. 1a, open symbols) due to a shift toward glycolysis and increased lactic acid extrusion, which is known as the Pasteur Effect (Winkler et al. 2004a, b). Indeed, it has been noted that retinal tissue has robust mitochondrial reserve capacity and, yet, also extrudes lactic acid indicative of significant anaerobic glycolytic flux (i.e., the Embden-Meyerhoff pathway coupled to pyruvate reduction via lactate dehydrogenase to oxidize NADH back to NAD^+) (Fox et al. 1999; Winkler et al. 2004a, b).

When looking at the OCR of 661W cells treated with oligomycin, FCCP, and antimycin A +rotenone, it is possible to quantify the amount of O_2 that is utilized by various bioenergetic processes. For instance, as shown in Fig. 1b, after treatment with oligomycin the OCR is decreased by the fraction of O_2 that is utilized by the mitochondrial ATP synthase for ADP phosphorylation, or the percentage of oxygen directed to OXPHOS. The mitochondrial reserve capacity is quantified as the difference between the FCCP-uncoupled OCR and the basal OCR, and any non-mitochondrial OCR is the residual OCR after treatment with antimycin A and rotenone. Finally, proton leak through the ETC can be calculated as the difference between the oligomycin rate (ATP production) and the antimycin A+rotenone OCR (non-mitochondrial O_2 consumption).

Effects of short-term calcium and oxidant stress on mitochondrial reserve capacity

Previous studies have shown that the degenerative process seen in, for example, the *rd1* mouse model induces changes in the bioenergetic metabolism that precedes cell death (Acosta et al. 2005; Lohr et al. 2006). The stressors generated by the effects of the gene mutation in the *rd1* photoreceptor, calcium and oxidant stress, have been shown to result in mitochondria-dependent cell death (Sharma and Rohrer 2004, 2007). To examine whether short-term calcium or oxidant stress results in changes in mitochondrial reserve capacity, the 661W cells were exposed to calcium ionophore, A23187 (500 nM), or the oxidant, tBuOOH (50 μM), on the XF24 instrument for 30 min, after which the treated cells were exposed to FCCP (1 μM) to uncouple the mitochondrial membrane potential and thereby estimate mitochondrial reserve capacity. Both A23187 and *t*BuOOH caused significant losses of mitochondrial reserve capacity 30 min after treatment as measured from the FCCP-uncoupled OCR (Fig. 2a – b) without affecting the basal rate. In separate experiments, after 30 min treatment with A23187 or tBuOOH, the cells were washed with PBS and then analyzed for cell viability via ethidium bromide/acridine orange staining. It was found that the cell viability 30 min after A23187 and *t*BuOOH treatments was >95 %, and not significantly different than vehicle-treated cells (data not shown). Thus, mitochondrial damage due to both calcium and oxidant stress are most evident as loss in the mitochondrial reserve capacity that is estimated from the maximal FCCP-uncoupled respiration rate. Similar observations have been reported for renal proximal tubular cells exposed to nephrotoxicants (Beeson et al. 2010).

Effects of long-term calcium and oxidant stress on cell survival and mitochondrial reserve capacity

The calcium ionophore, A23187, and oxidant, *t*BuOOH, are relatively non-specific, brusque stressors unlike the more subtle, chronic oxidant and calcium stressors seen in degenerative processes. To induce calcium stress in photoreceptor cells, which is more physiologically relevant, we and others have used IBMX, a non-selective phosphodiesterase (PDE) inhibitor that most likely targets photoreceptor phosphodiesterase (PDE6) in the 661W cells, (Zhang et al. 2005) although it may have additional off-target effects. Inhibition of PDEs cause increases in the intracellular cAMP and cGMP concentrations. In photoreceptors, increase in cGMP leads to persistent opening of the cGMP-gated cation channels and thus an increase of Ca^{2+} flux into the cell (Koutalos and Yau 1996; Yarfitz and Hurley 1994); and exposure of photoreceptor cells to 5 mM IBMX causes decreased response amplitudes and

desensitization of the cells similar to the effects of long-term Ca^{2+} treatment (Lipton et al. 1977). IBMX has also been shown to trigger a transient elevation of intracellular Ca^{2+} by releasing Ca^{2+} from intracellular stores in neurons (Usachev and Verkhratsky 1995). Treatment of 661W cells with IBMX transiently increases intracellular Ca^{2+} (Sharma and Rohrer 2004), although it is not clear as to the source of the Ca^{2+}. Paraquat (PQ) is a divalent bipyridinium cation, known primarily for its use as an herbicide. PQ crosses cell and mitochondrial membranes based on membrane potential, and it is reduced at complex I of the mitochondrial membrane (Cocheme and Murphy 2008). Upon reduction, a paraquat radical cation is formed, which rapidly reacts with oxygen to form superoxide (Hassan 1984), a primary source of intracellular oxidative stress. Upon reduction of oxygen, the paraquat is regenerated. Thus, paraquat is an intracellular redox cycler that simulates in vivo conditions of oxidative stress caused by excessive electron leak from complex I (Fukushima et al. 2002).

Initial experiments suggested that 24 h treatments with IBMX or PQ were needed to observe mitochondrial dysfunction. To determine concentrations that could be used without causing any cell death, the cells were incubated with a range of IBMX and PQ concentrations for 24 h, after which the cells were stained with propidium iodide and Hoechst 33342, and then imaged with an IN Cell automated cell imager. The Hoechst dye is plasma membrane permeable and stains nuclei of both live and dead cells whereas propidium only stains the nuclei of cells that have lost plasma membrane integrity (Fig. 3a,b). The subsequently determined dose responses (Fig. 3c,d) established that the maximal concentrations to be used for IBMX and PQ that did not induce cell death at 24 h were 0.6 mM and 0.5 mM, respectively. As previously shown (Sharma and Rohrer 2004, 2007), the extent of cell death was increased substantially after treatment for 48 h (Fig. 3c,d).

It should not come as a surprise that long-term (≥24 h) calcium and oxidant stress result in a significant loss of mitochondrial reserve capacity. The 661W cells were incubated with a range of concentrations of IBMX and PQ for 24 h after which the cells were washed, placed in DMEM media and their FCCP-uncoupled rates were measured with the XF24 analyzer. We found that both IBMX and PQ produce the same types of loss in mitochondrial reserve capacity as observed with the more potent, direct stressors, tBuOOH and A23187 (Fig. 4). However, while IBMX does not cause any measureable cell death when used below a concentration of 3 mM, maximal mitochondrial respiration is suppressed at 10-fold lower concentrations. The same is true for PQ, requiring 1 mM and higher to cause measurable cell death by 24 h, but only 0.5 mM to suppress maximal mitochondrial respiration by ~40 % (Fig. 4b).

Early effects on maximal mitochondrial respiration are predictive of cell death

Exposure to a range of concentrations of A23187 or *t*BuOOH for 30 min caused losses in mitochondrial reserve capacity, measured as attenuation of the FCCP-uncoupled OCR, or as increased ECAR in response to FCCP (the Pasteur Effect) (Fig. 2a,b). Although no cell death was evident after the acute 30 min treatments (data not shown), we also measured live cell numbers after 24 h treatment with A23187 or tBuOOH using the propidium iodide/ Hoechst 33342 imaging assay described and illustrated above (Fig. 3a,b). To determine the

correlation between changes in OCR and ECAR following FCCP exposure, and changes in the number of live cells, these three measurements were plotted versus the concentration of A23187 or *t*BuOOH (Fig. 5a,b). It was found that both the calcium and oxidant stresses produced very similar correlations between these two measures of metabolic changes in OCR and ECAR, due to uncoupling measured 30 min post stress treatment, and cell viability measured via dye exclusion at 24 h. In both cases, decreases in the FCCP uncoupled OCR values measured 30 min post-treatment in live cells are predictive of cell death at 24 h. Interestingly, at intermediate concentrations of stressor, the post-FCCP ECAR rate is substantially increased relative to basal, while the OCR has decreased. At higher concentrations the cells do not mount a Pasteur Effect (increased ECAR) and it is at these concentrations that extensive cell death is observed 24 h later.

The 661W cells were also treated with various concentrations of IBMX and PQ for 24 h after which metabolic measurements were made and the numbers of live cells were determined at 48 h post-treatment. Again, a plot of the changes in OCR (24 h), ECAR (24 h), and number of live cells (48 h) as a function of IBMX concentration demonstrates that loss in mitochondrial reserve capacity measured 24 h post-treatment in live cells, is predictive of cell death measured 48 h post-treatment (Fig. 5c). Also seen is the increase in ECAR at intermediate concentrations of IBMX (Fig. 5c). PQ, however, demonstrates a distinctly different pattern of OCR and ECAR response to FCCP following 24 h PQ exposure. The post-FCCP OCR values decrease with increasing PQ concentration, but there are no increases in ECAR, and cell death at 48 h is only observed at very high concentrations (Fig. 5d).

Discussion

The main results of the current study are 1) 661W cells are a good neuronal-like model that exhibit both mitochondrial respiration and glycolytic capacity; 2) short-term calcium and oxidant stress impair maximum mitochondrial reserve capacity without affecting basal respiration rates; 3) the degree of early impairment of mitochondrial reserve capacity correlates with the degree of cell death 24 h later; and 4) these concepts should be explored for the development of neuroprotective agents.

Here we wished to explore if defects in mitochondrial ATP-production may underlie neuronal pathology. We chose a photoreceptor cell line because of the retina’s high energy demand, damage caused by stressors such as calcium overload or reactive oxygen species is frequent in this tissue (Fox et al. 1999; Jarrett et al. 2008; Sharma and Rohrer 2004). While the RPE layer can absorb and metabolize some of this damage, it is thought that accumulation of damage outpaces the detoxification ability over time, eventually leading to the degenerative effects expressed in AMD and other retinopathies (Beckman and Ames 1998; Brand 2000; Brand and Nicholls 2011). One hypothesis is that this damage often occurs at the mitochondrial level (Jarrett et al. 2008), and it has been estimated that approximately 90 % of ROS originate from within the mitochondria (Balaban et al. 2005). Deletions in mitochondrial DNA resulting from ROS oxidation have been shown to increase with age (Mecocci et al. 1993; Richter 1988; Shigenaga et al. 1994), and an age-correlated decrease in mitochondrial membrane potential has also been observed (Hagen et al. 1997),

suggestive of ROS alteration of mitochondrial membrane phospholipids as well (Hoch 1992). Therefore, a plausible scenario for the initiation of pathology might include cells that require increased energy demand to detoxify harmful species like ROS, but are impaired from doing so because of preexisting damage, leading to inefficiency in the detoxification process; or the respiratory chain may be damaged in such a way that it generates predominantly free-radicals instead of ATP. Both of these scenarios create a “vicious cycle” resulting in even more damage (Bandy and Davison 1990; de Grey 2006; Miquel 1992). Our goal was to use extracellular flux measurements to show that damage to mitochondria leads to decreased maximum respiratory rate (i.e., the FCCP-uncoupled OCR) in a photoreceptor cell line as a model for retinal degeneration.

Here, we used the XF24 instrument to measure mitochondrial metabolism in retina-derived cells. Classically, oxygen consumption rates were measured in isolated tissues using Clark electrodes (e.g., (Ames et al. 1992)), or oxygen tension was determined in tissues or intact animals using oxygen sensitive electrodes (e.g., (Linsenmeier and Braun 1992)). In addition, ATP consumption by rod photoreceptors has been estimated by Okawa and colleagues (Okawa et al. 2008) based on the known voltages and currents, as well as physiological and biochemical data. In photoreceptors, just like other neuronal cell types, the majority of the ATP expenditure is utilized for ion extrusion to maintain membrane potential; whereas ATP required for biological processes such as protein synthesis and degradation or protein trafficking are negligible (e.g., Ames et al. 1992). Oxygen consumption in 661W cells as determined by XF24 is expected to be lower than in intact tissues primarily because the cells are not doing any meaningful work (i.e., light-induced signal transduction). However, as illustrated in Fig. 1, the 661W cells do have an appreciable level of aerobic metabolism. For example, the ~50 % reduction in OCR following treatment with oligomycin indicates that much of the respiration is directly coupled to ATP turnover, and this fractional decrease is comparable to what is seen with intact tissues (Lynch and Balaban 1987). Similarly, the approximately 1.5- to 2-fold increase in OCR relative to basal OCR following uncoupling with FCCP is comparable to increases observed in intact tissues and primary cells (Gandhi et al. 1995; Lynch and Balaban 1987; Stackley et al. 2011). Thus, utilization of the 661W cells with the XF24 instrument provides a useful method to evaluate the effect of stressors on cell bioenergetics.

The results illustrated in Fig. 5 demonstrate how the metabolic flexibility of the 661W cells can enable the cells to initially adapt to the calcium or oxidant stress before succumbing to cell death. The loss of mitochondrial reserve capacity, estimated as the decrease in the maximal FCCP-uncoupled rate, is predictive of calcium- or oxidant-induced cell death at later time points. Notably, at intermediate concentrations of A23187, tBuOOH, or IBMX, where cell death is still not observed at 24 h, the ECAR increase is suggestive of increases in glycolytic rates that are presumably attempts by the cells to compensate for loss of mitochondrial ATP. A Pasteur Effect was not observed for PQ treatment, but PQ is fundamentally different than a direct oxidant, such as *t*BuOOH, in that it invokes additional metabolic demand due to reduction-oxidation cycling. Thus, it could reduce maximal respiration partly due to damage and partly due to siphoning of electron chain flux, causing the apparent decrease in OCR to be magnified. A similar observation regarding increased

glycolytic rates prior to the onset of cell death was made when analyzing mRNA levels for 6-phospho-fructokinase (6-PFK) during photoreceptor degeneration in mouse models in which photoreceptor degeneration is triggered by calcium (*rd1*) or light damage. Prior to cell death, 6-PFK levels are elevated presumably to generate ATP to protect the cells against the ionic imbalance, but during cell death, 6-PFK levels are suppressed (Lohr et al. 2006). The increase and subsequent decrease of 6-PFK expression tracks with the changes in ECAR measured in 661W cells. Medrano and Fox (Medrano and Fox 1995) have shown that IBMX, in a manner that required the influx of extracellular Ca^{2+}, decreased basal OCR in acutely isolated rat photoreceptors. The decrease in basal OCR cannot arise from a decrease in ATP-consuming processes (i.e., inhibition of cGMP-PDE increases energy demand by maintaining the cyclic nucleotide-gated channel in the open state), but rather is due to a direct effect of Ca^{2+}, inhibiting mitochondrial oxygen consumption and ATP production.

Conclusion

We recognize that this study uses the 661W cell line, which has been cloned from a retinal tumor. Nevertheless this cell line has been used to recapitulate certain aspects of photoreceptor degeneration (Finnegan et al. 2010; Krishnamoorthy et al. 1999; Sharma and Rohrer 2004, 2007), and cellular and mitochondrial metabolism experiments share strong similarities with intact retinas (Ames et al. 1992; Medrano and Fox 1995). Given that the bioenergetic changes observed with calcium- and oxidant-mediated stressors recapitulate the changes seen in physiologically relevant models, we propose that the 661W photoreceptor model could be used to develop therapeutic strategies to mitigate photoreceptor cell dystrophies. We also propose that extracellular flux measurements provide perhaps the best way to measure mitochondrial dysfunction due to calcium- or oxidant-induced stress; and because many diseases have a mitochondrial liability that precedes cell death, this instrument will be a valuable aide in drug screening of chemical libraries to identify agents for the treatment of retinal, and in general neurodegenerative, pathologies.

Acknowledgements

This work was supported in part by National Institutes of Health grant EY013520, EY019320 (B.R.), a Department for Veterans Affairs merit award RX000444 (B.R.), the WG-TRAP award by Foundation Fighting Blindness (B.R. and C.B.), and an unrestricted grant to MUSC from Research to Prevent Blindness (RPB), New York, NY. B.R. is a RPB Olga Keith Wiess Scholar.

We thank John French for his initial contributions on applying the Cytosensor® microphysiometer technology to examine 661W cell metabolism, Gyda Beeson for her help with tissue culture, and Luanna Bartholomew for critical review.

References

Acosta ML, Fletcher EL, Azizoglu S, Foster LE, Farber DB, Kalloniatis M. Mol Vis. 2005; 11:717–728. [PubMed: 16163270]

Ames A 3rd, Li YY, Heher EC, Kimble CR. J Neurosci. 1992; 12:840–853. [PubMed: 1312136]

Balaban RS, Nemoto S, Finkel T. Cell. 2005; 120:483–495. [PubMed: 15734681]

Bandy B, Davison AJ. Free Radic Biol Med. 1990; 8:523–539. [PubMed: 2193852]

Beckman KB, Ames BN. Physiol Rev. 1998; 78:547–581. [PubMed: 9562038]

Beeson CC, Beeson GC, Schnellmann RG. Anal Biochem. 2010; 404:75–81. [PubMed: 20465991]

Brand MD. Exp Gerontol. 2000; 35:811–820. [PubMed: 11053672]

Brand MD, Nicholls DG. Biochem J. 2011; 435:297–312. [PubMed: 21726199]

Brand MD, Affourtit C, Esteves TC, Green K, Lambert AJ, Miwa S, Pakay JL, Parker N. Free Radic Biol Med. 2004; 37:755–767. [PubMed: 15304252]

Cocheme HM, Murphy MP. J Biol Chem. 2008; 283:1786–1798. [PubMed: 18039652]

Cruickshanks KJ, Klein R, Klein BE. Arch Ophthalmol. 1993; 111:514–518. [PubMed: 8470986]

de Grey AD. Free Radic Res. 2006; 40:1244–1249. [PubMed: 17090413]

Dranka BP, Hill BG, Darley-Usmar VM. Free Radical Biol Med. 2010; 48:905–914. [PubMed: 20093177]

Dranka BP, Benavides GA, Diers AR, Giordano S, Zelickson BR, Reily C, Zou L, Chatham JC, Hill BG, Zhang J, Landar A, Darley-Usmar VM. Free Radical Biol Med. 2011; 51:1621–1635. [PubMed: 21872656]

Finnegan S, Mackey AM, Cotter TG. Eur J Neurosci. 2010; 32:322–334. [PubMed: 20636478]

Fliesler SJ, Richards MJ, Miller CY, McKay S, Winkler BS. Exp Eye Res. 1997; 64:683–692. [PubMed: 9245897]

Fox DA, Poblenz AT, He L. Ann N Y Acad Sci. 1999; 893:282–285. [PubMed: 10672249]

Fukushima T, Tanaka K, Lim H, Moriyama M. Environ Health Prev Med. 2002; 7:89–94. [PubMed: 21432289]

Gandhi V, Estey E, Du M, Nowak B, Keating MJ, Plunkett W. Clin Cancer Res. 1995; 1:169–178. [PubMed: 9815970]

Grimm C, Wenzel A, Hafezi F, Yu S, Redmond TM, Reme CE. Nat Genet. 2000; 25:63–66. [PubMed: 10802658]

Hagen TM, Yowe DL, Bartholomew JC, Wehr CM, Do KL, Park JY, Ames BN. Proc Natl Acad Sci USA. 1997; 94:3064–3069. [PubMed: 9096346]

Hassan HM. Methods Enzymol. 1984; 105:523–532. [PubMed: 6328203]

Hoch FL. Biochim Biophys Acta. 1992; 1113:71–133. [PubMed: 1550861]

Jarrett SG, Lin H, Godley BF, Boulton ME. Prog Retin Eye Res. 2008; 27:596–607. [PubMed: 18848639]

Koutalos Y, Yau KW. Trends Neurosci. 1996; 19:73–81. [PubMed: 8820871]

Krishnamoorthy RR, Crawford MJ, Chaturvedi MM, Jain SK, Aggarwal BB, Al-Ubaidi MR, Agarwal N. J Biol Chem. 1999; 274:3734–3743. [PubMed: 9920926]

Linsenmeier RA, Braun RD. J Gen Physiol. 1992; 99:177–197. [PubMed: 1613482]

Lipton SA, Rasmussen H, Dowling JE. J Gen Physiol. 1977; 70:771–791. [PubMed: 201724]

Lohr HR, Kuntchithapautham K, Sharma AK, Rohrer B. Exp Eye Res. 2006; 83:380–389. [PubMed: 16626700]

Lynch RM, Balaban RS. Am J Physiol. 1987; 252:C225–C231. [PubMed: 3030121]

Mecocci P, MacGarvey U, Kaufman AE, Koontz D, Shoffner JM, Wallace DC, Beal MF. Ann Neurol. 1993; 34:609–616. [PubMed: 8215249]

Medrano CJ, Fox DA. Exp Eye Res. 1995; 61:273–284. [PubMed: 7556491]

Miquel J. Mutat Res. 1992; 275:209–216. [PubMed: 1383762]

Nichols WW, Epstein BJ. Curr Pharm Des. 2009; 15:304–320. [PubMed: 19149620]

Okawa H, Sampath AP, Laughlin SB, Fain GL. Curr Biol. 2008; 18:1917–1921. [PubMed: 19084410]

Redinbaugh MG, Turley RB. Anal Biochem. 1986; 153:267–271. [PubMed: 3706710]

Richter C. FEBS Lett. 1988; 241:1–5. [PubMed: 3197826]

Sharma AK, Rohrer B. J Biol Chem. 2004; 279:35564–35572. [PubMed: 15208318]

Sharma AK, Rohrer B. Curr Eye Res. 2007; 32:259–269. [PubMed: 17453946]

Shigenaga MK, Hagen TM, Ames BN. Proc Natl Acad Sci USA. 1994; 91:10771–10778. [PubMed: 7971961]

Smith PK, Krohn RI, Hermanson GT, Mallia AK, Gartner FH, Provenzano MD, Fujimoto EK, Goeke NM, Olson BJ, Klenk DC. Anal Biochem. 1985; 150:76–85. [PubMed: 3843705]

Stackley KD, Beeson CC, Rahn JJ, Chan SS. PLoS One. 2011; 6:e25652. [PubMed: 21980518]

Tan E, Ding XQ, Saadi A, Agarwal N, Naash MI, Al-Ubaidi MR. Invest Ophthalmol Vis Sci. 2004; 45:764–768. [PubMed: 14985288]

Tuszynski GP, Murphy A. Anal Biochem. 1990; 184:189–191. [PubMed: 2321754]

Usachev Y, Verkhratsky A. Cell Calcium. 1995; 17:197–206. [PubMed: 7542569]

Winkler BS, Arnold MJ, Brassell MA, Sliter DR. Invest Ophthalmol Vis Sci. 1997; 38:62–71. [PubMed: 9008631]

Winkler BS, Arnold MJ, Brassell MA, Puro DG. Invest Ophthalmol Vis Sci. 2000; 41:3183–3190. [PubMed: 10967082]

Winkler BS, Sauer MW, Starnes CA. Exp Eye Res. 2003; 76:715–723. [PubMed: 12742354]

Winkler BS, Sauer MW, Starnes CA. J Neurochem. 2004a; 89:514–525. [PubMed: 15056294]

Winkler BS, Starnes CA, Sauer MW, Firouzgan Z, Chen SC. Neurochem Int. 2004b; 45:311–320. [PubMed: 15145547]

Wu M, Neilson A, Swift AL, Moran R, Tamagnine J, Parslow D, Armistead S, Lemire K, Orrell J, Teich J, Chomicz S, Ferrick DA. Am J Physiol Cell Physiol. 2007; 292:C125–C136. [PubMed: 16971499]

Wu S-B, Wei Y-H. Biochim Biophys Acta. 2012; 1822:233–247. [PubMed: 22001850]

Yarfitz S, Hurley JB. J Biol Chem. 1994; 269:14329–14332. [PubMed: 8182033]

Yoshida Y, Singh I, Darby CP. Acta Neurol Scand. 1992; 85:191–196. [PubMed: 1575002]

Zglinicki, Tv. Aging at the molecular level Kluwer, Dordrecht. 2003

Zhang X, Feng Q, Cote RH. Invest Ophthalmol Vis Sci. 2005; 46:3060–3066. [PubMed: 16123402]

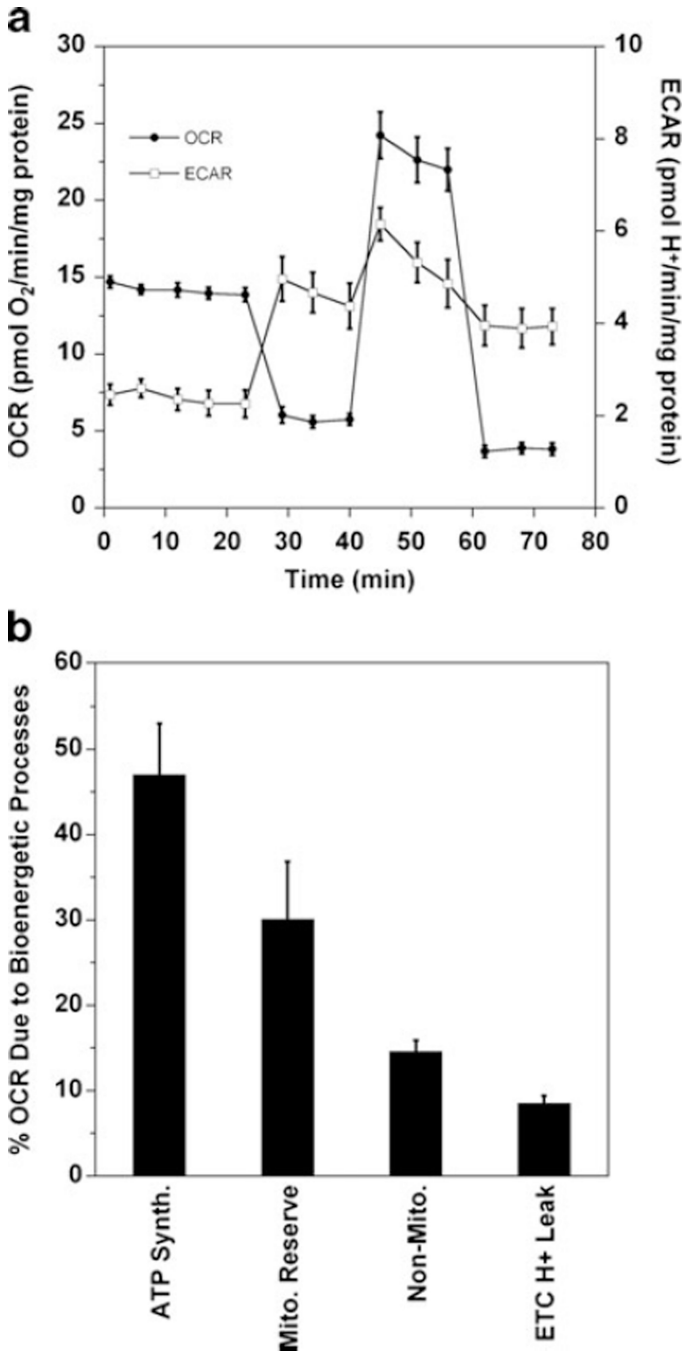

Fig. 1.

The 661W cells exhibit both mitochondrial respiration and glycolytic capacity. **a** The O_2 consumption rates (OCR) and extracellular acidification rates (ECAR) of 661W cells were measured with an XF24 Seahorse Biosciences instrument. The media is DMEM with 5.5 mM glucose; and the rates have been normalized to mg of protein. After measuring several basal rates, the cells were sequentially treated with oligomycin (0.5 μM), FCCP (1 μM), and antimycin A (500 nM)+rotenone (500 nM). Shown are the average rates±SEM for the group of wells at each time point (typically 3–5 wells/group). **b** Quantification of the oxygen

consumption due to various mitochondria-related bioenergetic processes in 661W cells, presented as a percentage of the total OCR observed after probing with oligomycin, FCCP, and antimycin A+rotenone. Mitochondrial ATP synthesis is the difference in the basal rate and the oligomycin OCR. Mitochondrial reserve capacity is the difference between the FCCP OCR and the basal rate, and non-mitochondrial OCR is any residual oxygen consumption after antimycin A and rotenone injection. ETC proton leak is calculated as the difference between the oligomycin OCR and the non-mitochondrial OCR. Each bar represents the average and SEM of 5 separate experiments with 3–5 wells/group

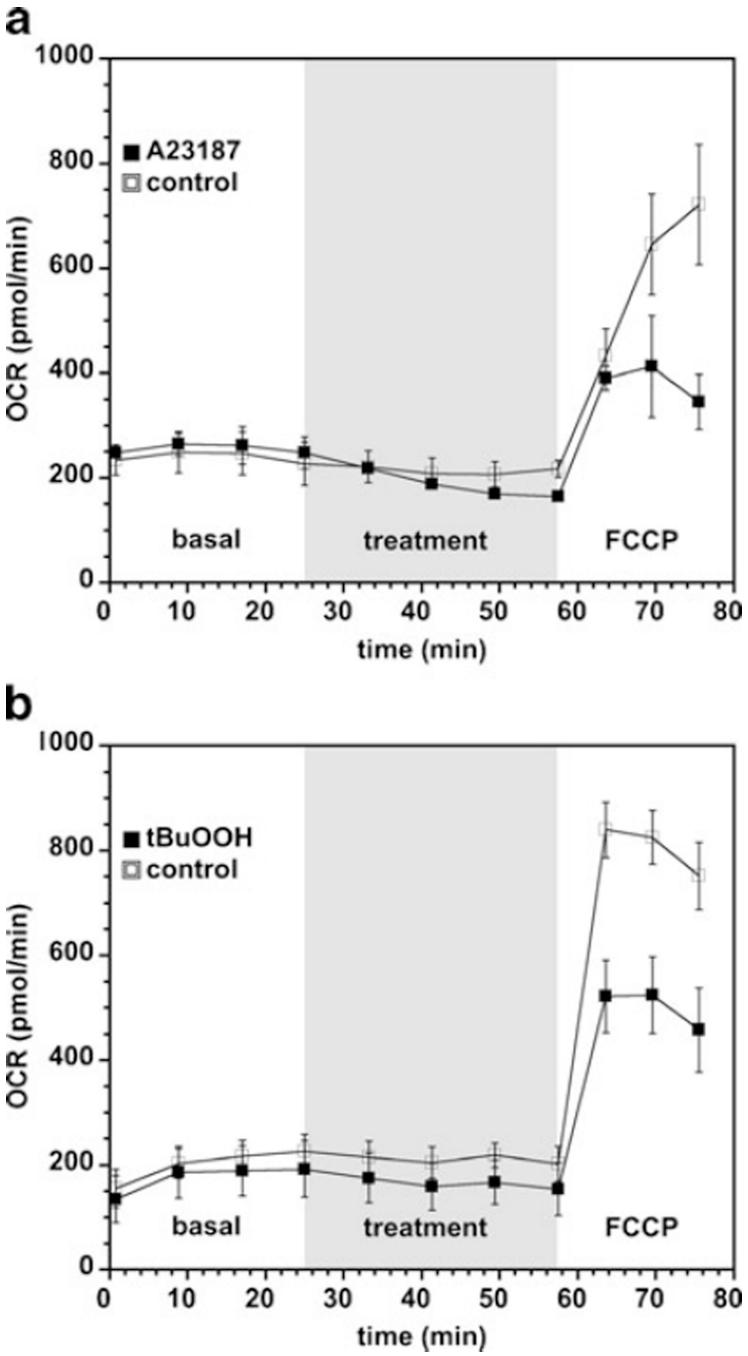

Fig. 2.

Short-term calcium and oxidative stress attenuate mitochondrial reserve capacity. Shown are representative 661W cell basal and FCCP-uncoupled OCR rates after treatment with (**a**) A23187 (500 nM) and (**b**) *t*BuOOH (50 μM). The shaded region of the chart shows when A23187, *t*BuOOH or vehicle solutions were injected prior to injection of FCCP. Results are the average OCR rates±SEM (*n*=3–4 experiments, 3 wells per experiment)

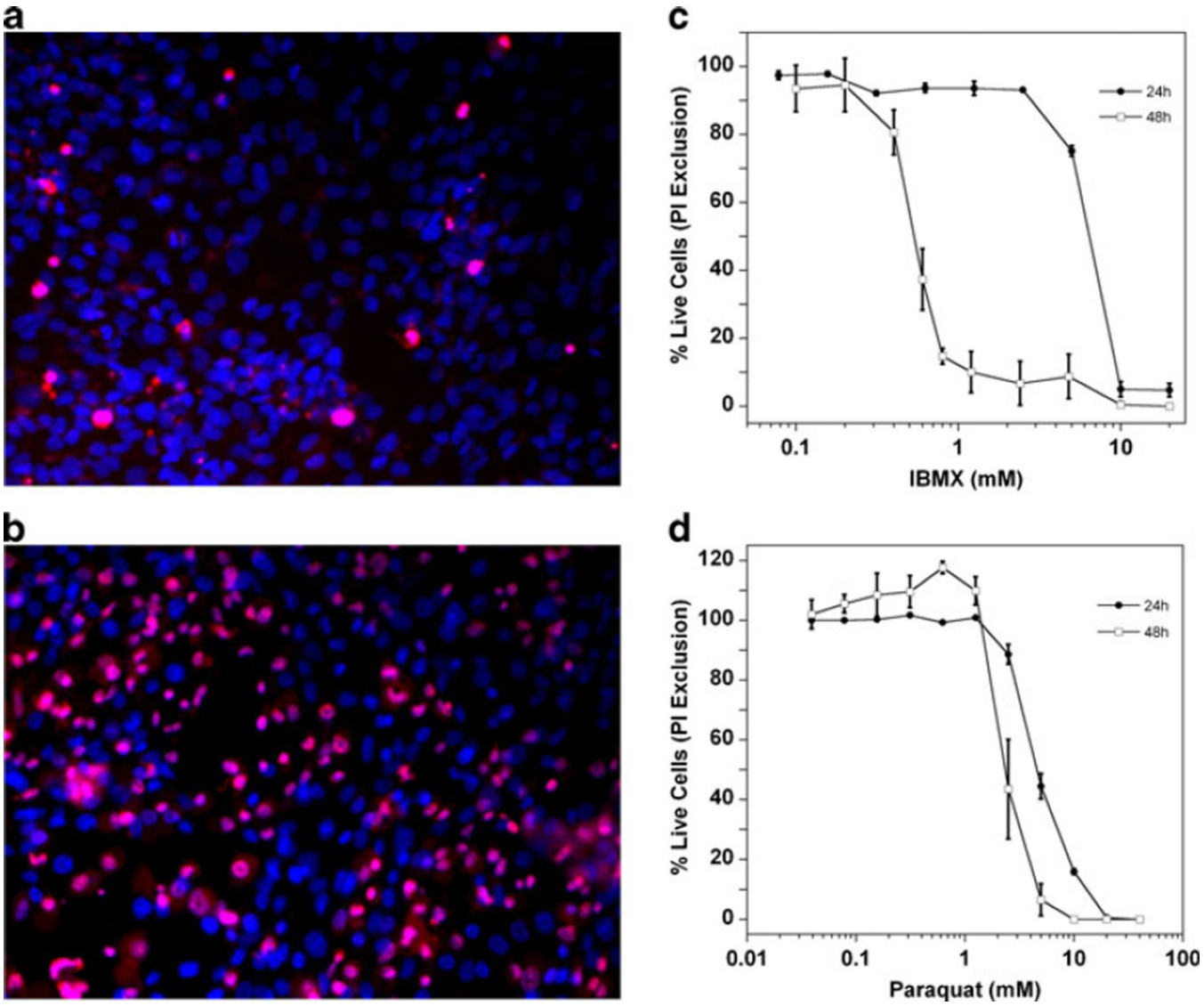

Fig. 3.

Live cell number dose-responses for 24 h treatment with A23187 and IBMX. Shown are representative images of 661W cells, obtained with a GE Health Sciences IN Cell 1,000 imager of cells stained with propidium iodide (dead cells, pink) and Hoechst 33342 (all cells, blue), treated with (**a**) vehicle control (0.5 % DMSO), and (**b**) 5 mM PQ for 24 h. Propidium iodide stained cells were subtracted from the total number of cells (Hoechst stained) to obtain the number of live cells and these values were normalized to control wells to obtain the percentage of live cells as a function of the concentration of IBMX (**c**) or paraquat (**d**)

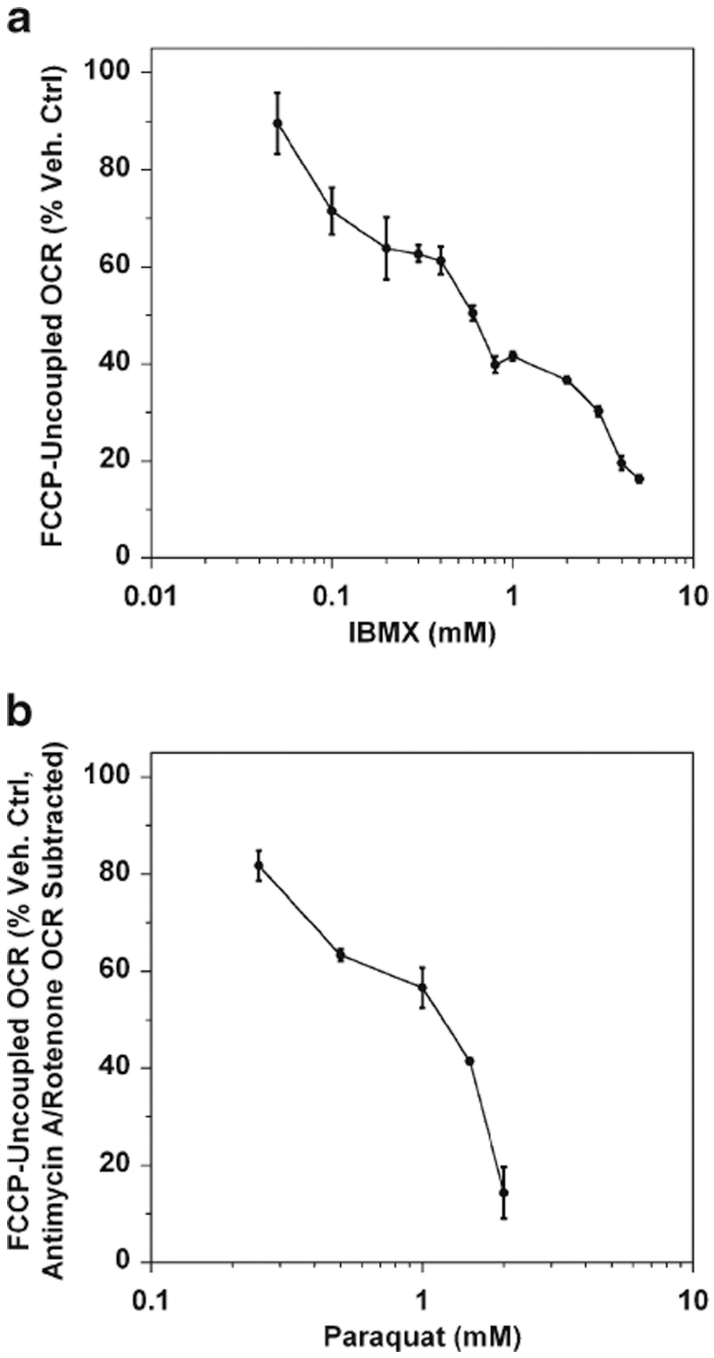

Fig. 4.

IBMX and paraquat impair mitochondrial reserve capacity after 24 h treatment. Shown are dose-dependent decreases in the mitochondrial reserve capacity (i.e., the FCCP-uncoupled respiration rates) for 661W cells treated for 24 h with IBMX (**a**) or PQ (**b**). Respiration rates are expressed as a percentage of vehicle control-treated cells±SEM (*n*=4–5 experiments, 3 wells per experiment). Note that the non-mitochondrial OCR was subtracted for PQ-treated cells because PQ itself consumes oxygen by redox cycling, causing a skewed OCR if this rate is not subtracted

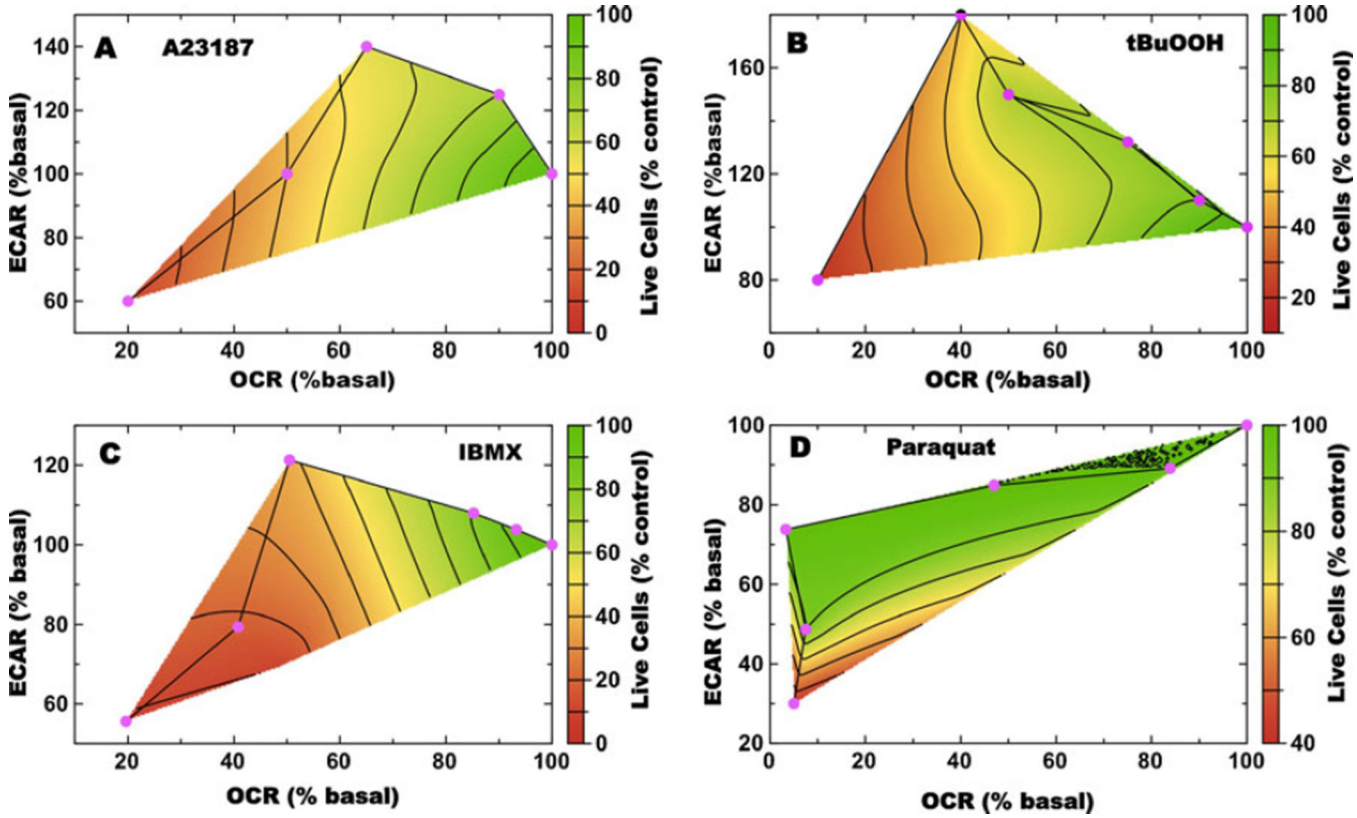

Fig. 5.

Calcium and oxidative stress produce metabolic phenotypes in 661W cells that are predictive of cell death. Shown in panels (**a**–**d**) are multivariate analyses of post-FCCP ECAR (y-axis), OCR (x-axis), and viability (z-axis, represented by color) for 661W cells treated with A23187 or *t*BuOOH for 30 min, or IBMX and PQ for 24 h. The concentrations of A23187 (**a**), *t*BuOOH (b), IBMX (c) and PQ (**d**) increase from right to left (cyan diamonds) and the metabolic rates are plotted as percentage change from basal